J Mol Model (2006) 12: 411–416
DOI 10.1007/s00894-005-0061-3

ORIGINAL PAPER

Christo Christov · Frederik Tielens · Miroslav Mirazchiiski

Modeling study of the influences of the aromatic transitions and the local environment on the far-UV rotational strengths in TEM-1 β-lactamase

Received: 21 February 2005 / Accepted: 26 July 2005 / Published online: 13 December 2005

Abstract Rotational strengths in the far-UV of TEM-1 β-lactamase have been investigated with two theoretical models based on the matrix method. The first model excludes, and a second includes, effects of the local electrostatic interactions on the chromophore energies. Special attention is given to the contributions of the aromatic side-chain chromophores, and the mechanisms of generation of rotational strengths are analyzed. The sensitivity of the computational models with respect to the structural changes of the protein are discussed.

Keywords Rotational strengths · Far-UV · β-lactamase TEM-1 · Matrix method · Environment effects · High-energy aromatic transitions

Introduction

β-Lactamases are enzymes that catalyze the hydrolysis of β-lactam antibiotics and are the major reason for bacterial resistance against them. β-Lactamase from *E. coli* **(TEM-1)** is a 29 kD protein that consists of one polypeptide chain, organized in two domains—all α and αβ. The X-ray structure of this protein has been determined by Jelsch et al. [1] (Fig. 1).

A very useful method for the investigation of the structure of biopolymers is Circular Dichroism (CD) [2]. The integrated intensity of à single CD band is proportional to the Rotational Strength (R), which is defined as the imaginary part of the scalar product between the vectors of the electric transition dipole moment and the magnetic transition dipole moment [3]:

$$R = \{\mu_{0i} \cdot m_{io}\} \tag{1}$$

where μ_{0i} and $\boldsymbol{m}_{i0}$ are the electric and magnetic transition moments of the 0→i electronic transition, respectively.

The mechanisms of generation of rotational strengths in proteins are: one-electron mechanisms or static-field effects [4]; the μ–μ mechanism [5, 6], which for the degenerate case is the exciton effect [7] and the μ-m mechanism [8]. For the detection of the changes in the secondary structure of the proteins, far-UV CD is a very appropriate technique [9]. The main contributions in far-UV are due to the peptide chromophores, but also to transitions of glutamates, aspartates, glutamines, asparagines, histidines, prolines and aromatic chromophores [10, 11]. The far-UV CD spectra of proteins have been the object of numerous computational studies [12–15]. Both experimental and calculated CD spectra of TEM-1 β-lactamase are known [16, 17] as well as the improvement of the calculated spectrum in the near-UV, the influences of the conformational changes, and electrostatic interactions on the near-UV rotational strengths [18–20]. The contributions of the aromatic side-chain chromophores to the far UV spectra have also been studied for several proteins [11, 13, 21, 22].

The electrostatic interactions determine to a large degree the conformations and the folding processes of proteins, and are also very important for the recognition and association processes, ligand binding, and enzyme catalysis [23–25]. Therefore, it is of utmost importance to understand the relationship between the electrostatic interactions and the chiroptical properties, which are representative for the changes in the secondary structure of proteins.

In the present paper we report a theoretical analysis of the relative differences of the mechanisms of the rotational strengths in the far-UV with both theoretical models based

C. Christov (✉)
Institute of Organic Chemistry,
Bulgarian Academy of Sciences,
Sofia, 1113, Bulgaria
e-mail: ch@orgchm.bas.bg

F. Tielens
Laboratoire de Chimie Théorique
Université Pierre et Marie Curie,
Case 137, 4 place Jussieu,
75252 Paris, Cedex 05, France

M. Mirazchiiski
Faculty of Biology,
University of Sofia "St. Kliment Ohridski",
1164 Sofia, Bulgaria

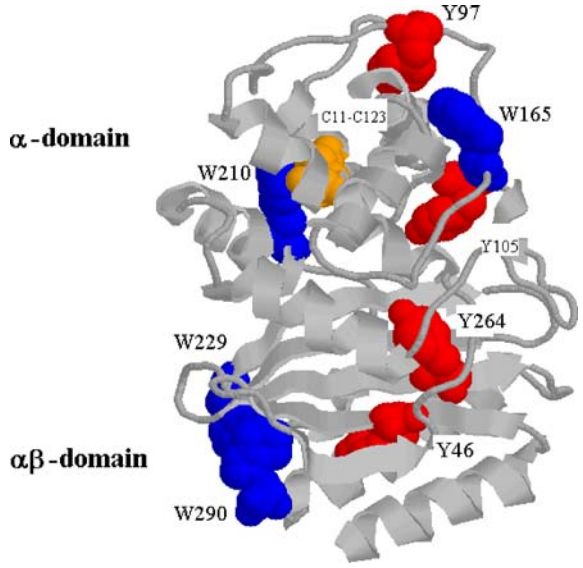

Fig. 1 Structure of TEM-1 β-lactamase. Both domains—α and αβ, the secondary structural elements and the aromatic and disulfide chromophores are shown

on the matrix method, presented elsewhere [26], i.e. with and without inclusion of the local environment around the chromophores in TEM-1 β-lactamase. Special attention is given to the contributions of the high-energy transitions of the aromatic chromophores to the far UV rotational strengths in order to give answers to the following questions: (1) How do the high-energy transitions of the aromatic chromophores (especially tryptophans) contribute the far-UV CD spectrum? (2) Which kind of mechanism for the generation of rotational strengths do they follow? (3) How are the aromatic, the other group contributions, and mechanisms influenced under the local electrostatic conditions? Furthermore, we provide a possible explanation on how both models express the sensitivity of the rotational strengths to conformational changes.

Materials and methods

The calculations of the rotational strengths were performed with the matrix method [26] in its origin-independent form [27], implemented in the program MATMAC, [28] kindly provided by Prof. Joerg Fleischhauer (RWTH-Aachen). This program has been used successfully to predict the CD spectra of numerous protein-like ribonuclease A, ribonuclease S [14], TEM-1 β-lactamase [17, 19], myoglobin, hemoglobin, lactate dehydrogenase, and other proteins [12], and peptides [29] in qualitative agreement with the experimental data.

The X-ray structures of the free enzyme and the protein components of four enzyme-ligand complexes were obtained from the Protein Data Bank [30]. For the free enzyme, the structure 1btl_pdb.ent was used [1]. The following structures of the enzyme-ligand complexes were used: the mutant, unable to deacylate (PDB code: 1fbg_pdb.ent) [31]; the complex with the inhibitor of deacylation stage—6α-(hydroxymethyl) penicilinic acid (PDB code: 1tem_pdb.ent) [32]; the enzyme-inhibitor complex with the acetylation inhibitor imepenem (PDB code: 1bt5_pdb.ent) [33] as well as the structure of the transition state analog of the acetylation stage (PDB code: 1axb_pdb.ent) [34].

The matrix method [26] considers the protein as a system of M independent chromophoric groups. The wave function of the macromolecular excited state is represented as a linear combination of the basis functions, including n_i excitations within each chromophoric group:

$$\Psi_k = \sum_{i}^{M} \sum_{a}^{ni} C_{ia}\phi_{ia} \tag{2}$$

Every basis function Φ_{ia} is a product from all M monomer wave functions.

The electronic excitation can arise in the groups, but not between them. In the basis functions, only one group can be in excited state.

In the Hamiltonian matrix:

$$H = \sum_{i=1}^{M} Hi + \sum_{i}^{M-1} \sum_{j=i+1}^{M} Vij \tag{3}$$

the diagonal elements are the energies of the excited states of the isolated chromophores, and the off-diagonal elements are of two types: the first one evaluates the interactions between different chromophoric groups and the second accounts for the mixing of the electronic transitions inside one chromophore under the influence of its environment. If the interactions between chromophores are considered as electrostatic, they can be written as:

$$Vi0a; j0b = \int_{ri}\int_{rj} \frac{\rho_{i0a}(\mathrm{ri})\rho_{i0b}(\mathrm{rj})}{4\pi\varepsilon_0 r_{i,j}} d\tau i\tau j, \tag{4}$$

where ρ_{i0a} and ρ_{i0b} are the permanent and transition electron densities of the transition 0→à in group i and for the transition 0→b in group j, respectively. The Hamiltonian matrix is diagonalized by unitary transformations. The diagonal elements in the new matrix are the excited states of the interacting system. The electric and magnetic dipole moments of the localized transitions in the chromophores are also diagonalized by the same unitary transformations in order to represent the interacting system. The imaginary part of the scalar product of them is the rotational strength of the whole protein.

The positions and charges of the monopoles for all chromophores with the exception of the tryptophans were used as in [14] the improved tryptophan chromophores were used as in [18].

The influences of local electrostatic interactions were estimated by including in the diagonal elements of the Hamiltonian matrix the energies of the excited states of the

isolated groups as well as their shifts under the local electrostatic interactions:

$$Hi = \Delta E_{i0a} + \sum_{i\neq} (V_{iaa;j00} - V_{i00;j00}) \quad (5)$$

where $V_{iaa;\,j00}$ is the Coulomb interaction between group i in excited state, and group j in ground state. $V_{i00;j00}$ is the interaction energy between both groups in ground state. The value of the effective dielectric constant was set to be one. To generate the CD-spectrum, the calculated rotational strengths were combined with Gaussian band-shape functions as in [14]. For the visualization of the structure of TEM-1 β-lactamase, the RasMol software was used [35].

Results and discussion

The experimental and calculated CD spectra of TEM-1 β-lactamase in the far UV without evaluation of the electrostatic interactions are shown in Fig. 2. The experimental spectrum consists in three bands: one positive at 190 nm and two negative at 208 and 220 nm. The first two result from the exciton splitting of the peptide ππ* transitions, which is characteristic for the α-helix. The maximum at 190 nm is due to electric transition dipole moments perpendicular to the helix axis, and the minimum at 208 nm to transition moments parallel to the helix axis [9]. The minimum at 220 nm is the result of peptide nπ*-transitions. The calculations with the matrix method without evaluation of local electrostatic contributions predict the maximum and the second minimum, but not the 208 nm minimum. The present calculations performed using improved monopoles for the tryptophan chromophores [18] led to a better agreement of the calculated CD spectrum of TEM-1 β-lactamase to experiment in the near-UV [19]. However, the 208 nm minimum is still missing in the calculated spectrum. Kurapkat et al. attribute this difference to the short lengths of the α-helices in ribonuclease A and ribonuclease S [14]. The facts that the lengths of the helices in TEM-1 β-lactamase are much larger, and that the magnitude of this minimum does not depend on the parameters for the tryptophans, confirm the suggestion that the reason for this discrepancy is that the angle between the electric transition moment of the NV1 peptide transition and carbonyl group used in these calculations is smaller than the experimentally determined one [17, 36]. Above 225 nm the major contributions are the peptide nπ*-transitions, B_b transitions of tryptophans and L_a transitions of tyrosines (Table 1). Because of the high complexity of the transitions below 225 nm the analysis of the mechanisms of generation of the rotational strengths is more difficult since the method was developed for transitions above this wavelength. Much better agreement to experiment is found within the interval 220–240 nm. The disulfide transitions do not contribute to the far-UV (Table 1). All known mechanisms for the generation of rotational strengths are shown in the interval 225–240 nm (Table 1). Exciton-like coupling between L_a transitions of Y46 and Y264 is found (transitions 4 and 5). Coupling of peptide nπ*-transitions with the L_a transition of Y105 could be assigned as the μ-*m* mechanism (transition 6). The one-electron effect is reproduced with the participation of both transitions of D157 (transition 1). The coupling interaction between both tryptophan chromophores (W229 and W290) is also recovered (transition 7). The calculations without tryptophans (Fig. 2, dotted line) led to smaller absolute values of rotational strengths, which prove that tryptophan chromophores contribute to the far-UV circular dichroism in TEM-1 β-lactamase.

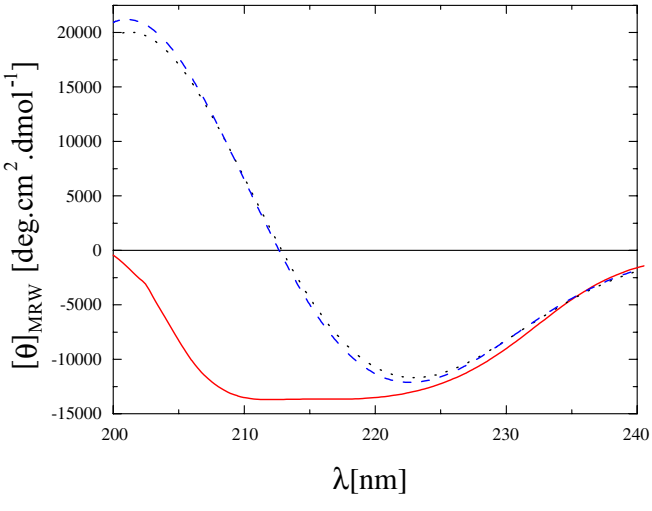

Fig. 2 Calculated and experimental spectra of TEM-1 β-lactamase in the far-UV without electrostatic interactions: *solid line*—experimental spectrum; *dotted line*—calculated without tryptophans; *dashed line*—calculated with tryptophans

Table 1 Calculated rotational strengths (225–240 nm) for TEM-1 β-lactamase without local electrostatic interactions

Transition	Local group contribution		Percent (%)	Wavelength (nm)	Rotational strength (DBM)
1	$n_1\pi^*$	D 157	50.00	–	–
	$n_2\pi^*$	D 157	49.99	230.90	−0.002
2	La	Y 105	57.27	–	–
	NV2	Pep 77	39.66	–	–
	nπ*	Pep 77	2.45	228.22	0.665
3	L_a	Y 97	99.25	227.38	0.027
4	L_a	Y 46	75.87	–	–
	L_a	Y 264	23.00	227.28	1.536
5	L_a	Y 264	76.43	–	–
	L_a	Y 46	22.85	227.14	−1.010
6	nπ*	Pep 77	55.04	–	–
	L_a	Y 105	41.89	–	–
	NV_2	Pep 77	2.49	226.07	0.631
7	nπ*	P 252	1.37	–	–
	B_b	W 229	61.35	–	–
	L_b	W 290	1.10	–	–
	B_b	W 290	32.57	–	–
	B_a	W 290	1.98	225.8	1.098

The effect of the local electrostatic environment on the far UV has been studied for ribonucleases A and S [14], which do not contain tryptophans. The electrostatic influence on the near-UV spectrum of the tryptophan-containing TEM-1 β-lactamase has also been analyzed [20]. The calculated spectrum including local Coulomb interactions in comparison to the experimental one is shown in Fig. 3. The method predicts the maximum, and the 220 nm minimum. However the 208 nm minimum could not be recovered. Both predicted maximum and minimum have smaller magnitudes than in the calculations without evaluation of electrostatic effects (Fig. 2). The peptide nπ* rotational strengths exhibit a strong long-wavelength displacement, which leads to an underestimation of the 220 nm peak (Table 2). In contrast to calculations without electrostatic effects, where they are concentrated around 220 nm they are spread up to 240 nm. The change of the electrostatic interactions of the chromophore with the adjacent groups from repulsive in the ground state to attractive in the excited state leads to a displacement of the transition to longer wavelengths.

Rotational strengths with the participation of histidine, asparagine and glutamine transitions (transitions 9, 12, 18, 22, 32, 34 and 36 in Table 2) are also displaced in a similar way. In contrast to the calculations without electrostatic interactions, the coupling between the La transitions of Y46 and Y264 is not found. The tryptophan high-energy transitions under electrostatic interactions generate rotational strength in a more complex manner with couplings with histidine transitions (transitions 36 and 40 in Table 2) than in the calculations without evaluation of the electrostatic energy shift (transition 7 in Table 1). The incorporation of the local electrostatic interactions also does not reproduce the 208 nm minimum in the far-UV, which supports our above-mentioned suggestion.

Nevertheless, that absence of the 208 nm minimum from our calculations with and without evaluation of the local environment, the relative difference, and the relative degree of perturbation of the rotational strength mechanisms under the above-mentioned effects have been analyzed. Reproducing the double minima (208 and 220 nm) is still challenging, and different strategies have been used to

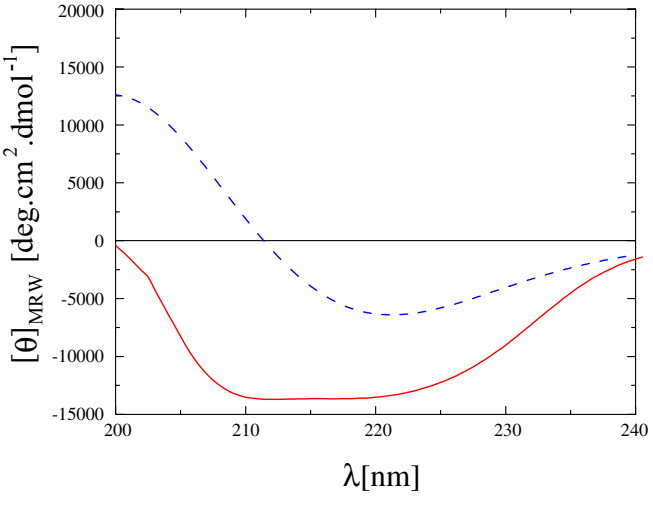

Fig. 3 Calculated spectrum in the far-UV for TEM-1β-lactamase with evaluation of the local electrostatic interactions: *solid line*—experimental spectrum; *dashed line*—theoretical spectrum including all chromophores

Table 2 Calculated rotational strengths (225–240 nm) for TEM-1 β-lactamase including local electrostatic interactions

Transitions	Local group contributions			Percent (%)	Wave-length (nm)	Rotational strength (DBM)
1	nπ*	–	Pep 98	98.94	239.62	−0.342
2	nπ*	–	Pep 76	99.95	235.95	0.041
3	nπ*	–	Pep 2	99.89	234.61	−0.088
4	nπ*	–	Pep 165	99.47	234.44	−0.175
5	nπ*	–	Pep 72	99.76	233.24	−0.125
6	nπ*	–	Pep 77	93.31	–	–
	NV2	–	Pep 77	4.02	233.19	0.180
	L_a	–	Y105	2.43	–	–
7	nπ*	–	Pep 31	99.67	232.86	−0.194
8	nπ*	–	Pep 202	99.99	232.27	−0.015
9	nπ*	–	Q 278	99.99	232.15	0.245
10	nπ*	–	Pep 16	99.98	231.75	−0.034
11	nπ*	–	Pep 1	99.86	230.43	−0.067
12	ππ*	–	H 153	99.39	230.02	0.203
13	L_a	–	Y 46	99.25	229.47	0.291
14	$n_2π^*$	–	D 157	50.69	–	–
	$n_1π^*$	–	D 157	49.3	229.36	0.012
15	nπ*	–	Pep 168	99.52	229.26	−0.212
16	nπ*	–	Pep 172	99.34	229.12	−0.238
17	nπ*	–	Pep 238	99.55	229.01	−0.243
18	nπ*	–	N 132	99.86	228.85	−0.024
19	n π*	–	Pep 97	99.33	228.63	−0.196
20	nπ*	–	Pep 164	99.91	228.39	−0.054
21	nπ*	–	Q 90	99.97	228.34	0.007
22	$ππ_1^*$	–	H 289	64.15	228.19	0.727
	$ππ_1^*$	–	H 26	34.76	–	–
23	nπ*	–	Pep 94	98.19	227.91	0.210
24	nπ*	–	Pep 68	99.53	227.74	−0.016
25	L_a	–	Y 264	99.46	227.7	0.152
26	nπ*	–	Pep 185	99.84	227.53	0.064
27	L_a	–	Y 97	97.82	227.31	0.141
28	nπ*	–	Pep 125	99.89	226.9	−0.019
29	nπ*	–	Pep 84	99.16	226.82	−0.018
30	L_a	–	Y 105	69.28	226.53	−0.335
	nπ*	–	Pep 200	28.21	–	–
	nπ*	–	Pep 77	1.75	–	–
31	nπ*	–	Pep 200	71.75	226.51	0.375
	L_a–	–	Y 105	27.23	–	–
32	nπ*	–	Pep 91	73.4	225.93	−0.102
	nπ*	–	Q 88	26.23	–	–
33	nπ*	–	Q 88	73.74	225.92	−0.002
	n π*	–	Pep 91	26.12	–	–
34	nπ*	–	N 154	99.83	225.61	−0.025
35	nπ*	–	P 183	99.64	225.59	−0.189

Table 2 (continued)

Transitions	Local group contributions			Percent (%)	Wave-length (nm)	Rotational strength (DBM)
36	Bb	–	W 290	29.29	225.32	2.076
	ππ1*	–	H 26	28.28	–	–
	Bb	–	W 229	19.49	–	–
	ππ 1*	–	H 289	15.58	–	–
	NV1	–	Pep 250	2.69	–	–
	Ba	–	W 290	1.57	–	–
	Lb	–	W 290	1.08	–	–
37	nπ	–	Pep 70	99.77	225.29	−0.120
38	n2 π*	–	D 233	52.09	225.17	−0.469
	n1π*	–	D 233	47	–	–
39	nπ*	–	Pep 113	99.91	225.16	0.028
40	ππ1*	–	H 26	33.45	225.02	−3.73
	Bb	–	W 229	25.55	–	–
	Bb	–	W 290	18.42	–	–
	ππ1*	–	H 289	18.09	–	–
	Ba	–	W 290	1.24	–	–

improve the calculations in the far UV [36, 37]. Despite the improvement of the model chromophores, there is still some more work to do to calculate CD quantitatively in the far-UV, such as the inclusion of the influence of the macromolecular environment.

The evaluation of the local environment influences the total contributions of the high-energy aromatic chromophores (Table 3). All transitions decrease their total rotational strengths and B_b transitions of tryptophans change their signs under the local environment.

In order to show how the rotational strengths in the far-UV with and without incorporation of the local environment are sensitive to the small conformational changes related to the catalytic cycle of the enzyme, and how the calculations depend on the choice of the initial structure, we have done calculations for four protein components of the enzyme-ligand complexes related to the catalytic cycle of the enzyme. The spectra in the interval 215–230 nm calculated with the classical matrix method are shown in Fig. 4. Despite that slightly larger magnitudes are found for the protein component of the acyl-enzyme structure, (1fqg.pdb) the spectra are comparable. In contrast, the calculated spectra including local electrostatic environments exhibit more sensitive dependence on the conformational changes (Fig. 5). In relation to our previous work [20] and our unpublished results we suggest that such a larger sensitivity

Table 3 Total contributions of aromatic and disulfide transitions, calculated without and including of the local electrostatic interactions in the interval 225–240 nm

Theoretical model	B_bW (DBM)	B_aW (DBM)	L_aY (DBM)
Without local environment	1.031	0.022	1.188
Including local environment	−0.627	0.013	0.453

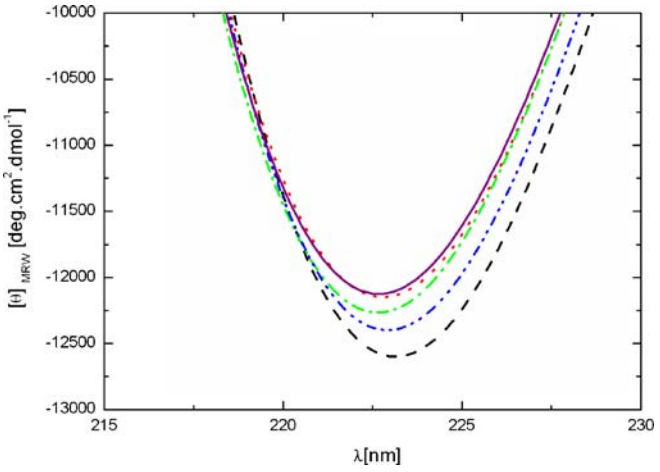

Fig. 4 Calculated spectra for the protein components of enzyme–ligand complexes without the local environment: *solid line*—spectrum of the free enzyme (1btl.pdb); *dashed line*—1fqg.pdb; *dotted line*—1tem.pdb; *dash–dot line*—1bt5.pdb; *dash–dot–dot line*—1axb.pdb

is related to the perturbation of high-energy aromatic rotational strengths by local electrostatic interactions.

It should be acknowledged that the calculations presented have the following simplifications: a) the lack of estimation of the structural dynamics and solvent effects, b) the chromophore monopoles are calculated for the models without evaluation of the environment, and c) the charge transfer between groups is not taken into account. The value of the effective dielectric constant used was one which can lead to larger energy shifts, however, the applicability of higher dielectric constant or distance-dependent dielectric constants cannot be strongly motivated. Different values for the dielectric constant inside the protein have been reported. The controversy arises because of different points of view about two kinds of phenomena, the screening of charge interactions in proteins and the "solvation" of charges when they are buried inside the

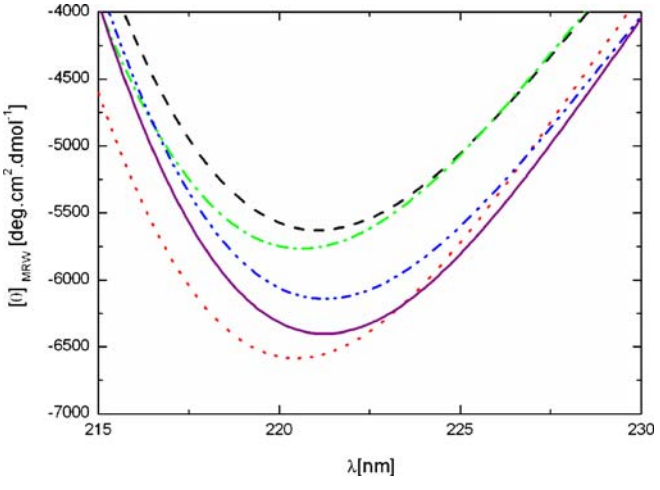

Fig. 5 Calculated spectra for the protein components of enzyme–ligand complexes including of the local environment: *solid line*—spectrum of the free enzyme (1btl.pdb); *dashed line*—1fqg.pdb; *dotted line*—1tem.pdb; *dash–dot line*—1bt5.pdb; *dash–dot–dotline*—1axb.pdb

protein [38]. The factors that determine the optimal value of this constant are far from obvious. It is shown that the protein dielectric constant is not a universal constant but simply a parameter that depends on the model used. The optimal value of the dielectric constant for self-energies is not the optimal constant for charge-charge interactions [39].

Independently of the above-mentioned drawbacks, the results presented explain by which mechanisms the high-energy aromatic transitions generate rotational strengths in the far-UV and how these mechanisms and contributions are influenced by local interactions of the chromophores with their surroundings.

Conclusions

Our results give qualitative insight into the mechanisms for the generation of rotational strengths in the far-UV in TEM-1 β-lactamase. They suggest that the evaluation of the electrostatic environment around the chromophores alter these mechanisms and can influence their sensitivity to conformational changes of the proteins.

The model presented can be used for a better understanding of the relationship between chiroptical properties, electrostatic interactions, and conformational changes related to the biochemical functions of the proteins.

Acknowledgements This work was supported by grant RIG-981486 from NATO and grant YS-CH-1202 from the Bulgarian Science Foundation. The authors are thankful to Prof. Joerg Fleischhauer (RWTH-Aachen, Germany), Prof. Juan Andres (University Jaume I, Castellon, Spain) for fruitful discussions.

References

1. Jelsch C, Mourey L, Masson JM, Samama JP (1993) Proteins 16:364–383
2. Cantor CR, Schimmel PR (1980) Biophysical Chemistry. Freeman WH and Company. San Francisco
3. Rosenfeld L (1928) Z Phys 52:161–174
4. Condon EU (1937) J Chem Phys 5:753–775
5. Kuhn W (1930) Trans Faraday Soc 46:293–308
6. Kirkwood JG (1937) J Chem Phys 5:479–491
7. Moffitt W, FItts DD, Kirkwood JG (1957) Proc Natl Acad Sci USA 43:723–730
8. Schellman J (1968) Acc Chem Res 1:144–151
9. Woody RW (1996) In: Fasman GD (ed) Circular dichroism and the conformational analysis of biomolecules. Plenum, New York p 25
10. Woody RW (1994) European Biophysics Journal with Biophysics Letters 23:253–262
11. Andrew CD, Bhattacharjee S, Kokkoni N, Hirst JD, Jones GR, Doig AJ (2002) J Am Chem Soc 124:12706–12714
12. Besley NA, Hirst JD (1999) J Am Chem Soc 121:9636–9644
13. Rogers DM, Hirst JD (2004) Chirality 16:234–243
14. Kurapkat G, Kruger P, Wollmer A, Fleischhauer J, Kramer B, Zobel E, Koslowski A, Botterweck H, Woody RW (1997) Biopolymers 41:267–287
15. Woody RW (2004) In: Energetics of Biological Macromolecules. Pt E, pp 242–285
16. Vanhove M, Raquet X, Frere JM (1995) Proteins 22:110–118
17. Christov C, Gabriel S, Atanasov B, Fleischhauer J (2001) Z Naturforsch A 56:757–760
18. Christov C (2002) Bulgarian Academy of Sciences. Sofia
19. Christov C, Karabencheva T (2004) Chem Phys Lett 396:282–287
20. Christov C, Kantardjiev A, Karabencheva T, Tielens F (2004) Chem Phys Lett 400:524-530
21. Grishina I, Woody RW (1994) Biophysical Journal 66:A376–A376
22. Sreerama N, Manning MC, Powers ME, Zhang JX, Goldenberg DP, Woody RW (1999) Biochemistry 38:10814–10822
23. Berendesen HJC (1993) In: Computer Simulations of Biomolecular Systems: Theoretical and Experimental Applications. Leiden, ESCOM
24. Honig B, Nicholls A (1995) Science 268:1144–1149
25. Nilsson JNL (2003) Quarterly Reviews of Biophysics 36:257–306
26. Bayley PM, Nielsen EB, Schellman JA (1969) J Phys Chem 73:228–243
27. Goux WJ, Hooker TM (1980) J Am Chem Soc 102:7080–7087
28. Fleischhauer J, Kramer B, Zobel E, Koslowski A (2000) MATMAC V2.0 Matrix and Tinoco method Program for the calculation of Rotational Stengths of Biopolymers. RWTH: Aachen
29. Fleischhauer J, Grotzinger J, Kramer B, Kruger P, Wollmer A, Woody RW, Zobel E (1994) Biophys Chem 49:141–152
30. Berman HM, Westbrook J, Feng Z, Gilliland G, Bhat TN, Weissig H, Shindyalov IN, Bourne PE (2000) Nucleic Acids Research 28:235–242
31. Strynadka NCJ, Adachi H, Jensen SE, Johns K, Sielecki A, Betzel C, Sutoh K, James MNG (1992) Nature 359:700–705
32. Maveyraud L, Massova I, Birck C, Miyashita K, Samama JP, Mobashery S (1996) J Am Chem Soc 118:7435–7440
33. Maveyraud L, Mourey L, Kotra LP, Pedelacq JD, Guillet V, Mobashery S, Samama JP (1998) J Am Chem Soc 120:9748–9752
34. Maveyraud L, Pratt RF, Samama JP (1998) Biochemistry 37:2622–2628
35. Sayle R, Milner-White EJ (1995) Trends Biochem Sci 20:374–376
36. Woody RW, Sreerama N (1999) J Chem Phys 111:2844–2845
37. Hirst JD (1998) J Chem Phys 111:782–788
38. Harvey SC (1989) Proteins: Struct Funct Genet 5:78–92
39. Schutz CN, Warshel A (2001) Proteins 44:400–417